AIAA JOURNAL
Vol. 33, No. 5, May 1995

Reynolds Number Effects in Swept-Shock-Wave/Turbulent-Boundary-Layer Interaction

A. W. C. Leung* and L. C. Squire†
Cambridge University, Cambridge CB2 1PZ, England, United Kingdom

The interaction between a turbulent boundary layer and a glancing shock wave produced by a wedge is studied numerically and experimentally. The flows correspond to a nominal Mach number 2.5, two widely different Reynolds numbers, and a range of incidence angles giving both attached and separated flows. The Reynolds number effects on several flow features, including upstream influence, incipient separation, and inception length, are discussed. The computations are compared with the low-Reynolds-number experiments of Kubota and Stollery and also to some newly performed high-Reynolds-number experiments, and good agreement is achieved.

I. Introduction

IN the last 15 years or so there has been intensive research on flows in which a shock wave produced by a wedge glances across the turbulent boundary layer on a wall perpendicular to the wedge, as shown in Fig. 1. Based on experimental and computational evidence, a number of investigators (i.e., Kubota and Stollery[1] and Alvi and Settles[2]) have proposed models for the overall flowfield, and a comprehensive overview of the whole field has been given by Settles and Dolling.[3] Among other flow features, incipient separation has attracted much attention since the onset of separation changes the flowfield considerably. Much effort has also been spent on studying the interaction pattern on the sidewall surface. Many investigators (e.g., Degrez and Ginoux[4] and Settles and Lu[5]) find that there exists an inception region near the wedge apex, beyond which the interaction conforms to a conical (or nearly so) pattern. Scaling laws (e.g., Settles[6] and Lu et al.[7]) have been devised to relate the inception length and upstream influence extent to more primitive flow variables such as the inviscid shock angle. The effects of the wedge angle and the freestream Mach number are well studied in these works. Certain effects of the Reynolds number have also been investigated and are summarized in Settles and Dolling[3]. In this paper we are particularly interested in the relatively weak interactions, and the objectives of the present paper are twofold: 1) to use results from two extensive experimental investigations to study the Reynolds-number effects on swept-shock-wave/turbulent-boundary-layer interactions at, and just above, incipient separation, and 2) to check if features of the two flows can be predicted by a Navier–Stokes solver using simple turbulence models.

About 25 years ago Lowrie,[8] in the Cambridge University Engineering Department, performed a series of experiments on the three-dimensional interactions. Because he chose a rather high stagnation pressure, the unit freestream Reynolds number in his flow was about 5×10^7/m. Later, Kubota and Stollery[1] conducted another experimental program in Cranfield with essentially the same configuration and at a similar Mach number. However, since the stagnation pressure was much lower than the one used by Lowrie, the Reynolds number in the two cases differ by an order of magnitude. These two works therefore should provide a good basis for investigation of the Reynolds-number effects on various aspects of the swept interaction. In particular, recently Lu,[9] Dou and Deng,[10] and Zheltovodov et al.[11] have developed prediction methods for incipient separation. All of these authors have compared their predictions with the available data. The experimental results show a large amount of scatter that is probably due to differences in the experimental techniques and the application of the criteria used to determine incipient separation. Thus the results of the comparisons are rather inconclusive. The Cambridge/Cranfield tests would appear to be ideal test cases to study the Reynolds-number effects on separation predicted by Dou and Deng and by Zheltovodov et al. Unfortunately, the wedge angle ranges in Lowrie's and Kubota and Stollery's cases do not overlap completely. Therefore a series of experiments has been performed by the present authors, using the same tunnel and freestream conditions as Lowrie but the wedge angles chosen by Kubota and Stollery. Moreover, the two flows at the different Reynolds-numbers are also simulated by a Navier–Stokes solver.

II. Details of Experiments

High Reynolds Number

The tunnel used in the present experiments is of the intermittent, blowdown type. Compressed gas was delivered to the tunnel working section, which measures 76.2 (wide) × 203.2 mm (high). The stagnation pressure and temperature were 0.515 ±0.014 MPa and 290 ± 4 K, respectively. The actual Mach number in this set of flows was 2.45 ±0.05. The freestream unit Reynolds number was 5.33×10^7/m. The 99.5% boundary-layer thickness was 5.6 ±0.15 mm. The displacement and momentum thicknesses were $\delta^* = 1.53$ ±0.04 mm and $\theta = 0.37$ ±0.01 mm, respectively.

Low Reynolds Number

The experiments were performed by Kubota and Stollery[1] in the Cranfield Institute of Technology. The tunnel cross section is 229-mm square. The total pressure and temperature were 27.9 ±1 kPa and 290 K, respectively. The actual Mach number was 2.3 ±0.05. The freestream unit Reynolds number was 3.07×10^6/m. The 99.5% boundary-layer thickness was 16.0 mm. The displacement and momentum thicknesses were $\delta^* = 3.8$ mm and $\theta = 1.0$ mm, respectively.

III. Details of Computation

The Navier–Stokes solver used was written by Dawes.[12] It solves the three-dimensional compressible Reynolds-averaged Navier–Stokes equations by an implicit finite volume scheme. In the present work, the flow is assumed to be isenthalpic because Holmes and Squire[13] have found that this assumption, while considerably reducing the necessary CPU time in the computation, does not significantly affect the accuracy in calculating shock-wave/turbulent-boundary-layer interactions.

The size of the meshes used in the calculations is 54 × 90 × 64 (x-y-z) and a typical grid is shown in Fig. 2. There is grid refinement towards the viscous surfaces (wedge and sidewall). The plane of cells adjacent to these boundaries always lies in the viscous sublayer of the boundary layer, with y^+ (or z^+) less than 5. The x-wise spacing is constant around the compression corner ($0.55\delta_\infty$ and $0.2\delta_\infty$ for the high- and low-Reynolds-number flows, respectively)

Presented as Paper 93-2937 at the AIAA 24th Fluid Dynamics Conference, Orlando, FL, July 6–9, 1993; received July 14, 1993; revision received May 9, 1994; accepted for publication Aug. 9, 1994.

*Graduate Student, Engineering Department. Member AIAA.
†Reader, Engineering Department. Fellow AIAA.

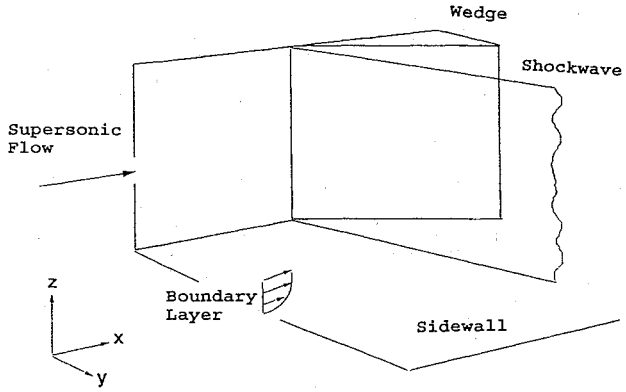

Fig. 1 Flow configuration.

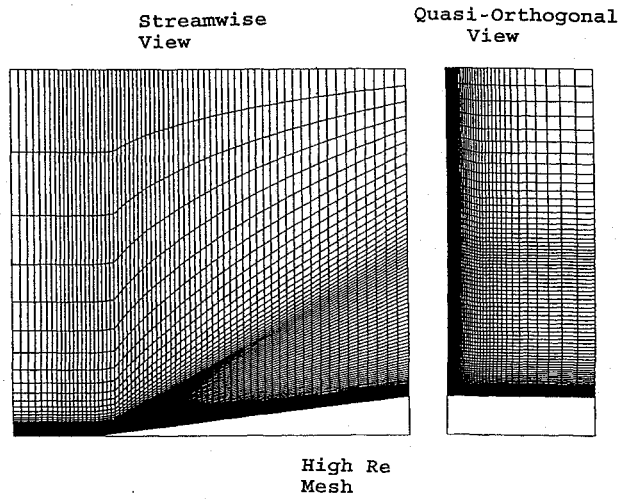

Fig. 2 Views of the meshes used in the calculations.

and expands towards the inlet and outlet. As in the work of Holmes and Squire,[13] the mesh is shock aligned to permit efficient shock capturing, as shown in the streamwise view in Fig. 2. From the quasi-orthogonal views, it is seen that the mesh is staggered (i.e., the shock-alignment angle changes) towards the sidewall. This is to provide better prediction of upstream influence in the interaction. From the computation of Holmes and Squire and our own work, it is considered that this grid form is very appropriate for the present problem, giving fine resolution to areas where necessary and producing stable and fast convergence. Moreover, further refinements of the grid were shown not to result in significantly different solutions. For the high-Reynolds-number flow, the domain extends from $4.4\delta_\infty$ (or 24.5 mm) upstream of the compression corner to $37.2\delta_\infty$ (or 206.8 mm) downstream of it. The dimensions of the domain in the y and z directions are $44.6\delta_\infty$ (or 250 mm) and $20\delta_\infty$ (or 111.2 mm), respectively. For the low-Reynolds-number case, the lengths of the domain upstream and downstream of the compression corner are $4.7\delta_\infty$ (or 75.1 mm) and $9.6\delta_\infty$ (or 152.4 mm), respectively. Moreover, it measures $23.6\delta_\infty$ (or 375 mm) and $15\delta_\infty$ (or 238.1 mm) in the y and z directions, respectively.

The Cebeci–Smith[14] and Johnson–King[15] turbulence models are used to provide closure. The length scale due to Buleev[16] is adopted in both models as the effective wall distance. The boundary-layer edge (Fig. 3) is located, in zones I and IV, approximately by searching along the y or z direction until the criterion $\Delta q/q < 0.002$ is satisfied by three consecutive cells. After the edge has been approximately found, a more exact search is performed in the neighboring few cells to locate the position where the total velocity q equals $0.99\times$ the value at the boundary edge. Near the wedge/sidewall junction, i.e., in zones II and III, the value of δ is treated as a constant equal to the Buleev distance of the b.l.edge/corner bisector intersection. This is similar to the methods of Hung and MacCormack[17] and Cambier and Escande.[18] A zonal approach is also applied to the evaluation of the displacement thickness. Since the boundary layers

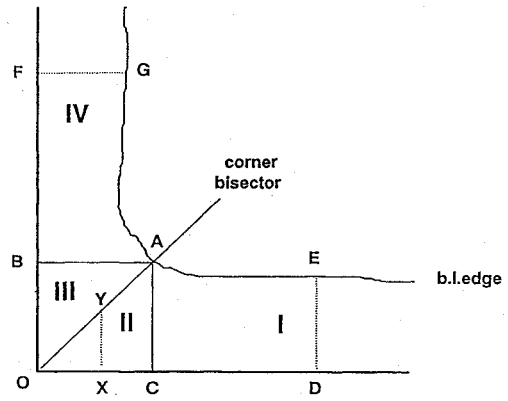

Fig. 3 Zonal approach for boundary-layer treatment.

in zones I and IV of Fig. 3 are along normals from walls, it is natural to set the normals to be the integration paths in these zones. Points on a normal are all assigned a δ_i^* value equal to the integral evaluated along the normal. In zones II and III, the integration path is a normal followed by a segment of the bisector, e.g., XYA. Sometimes the maximum velocity along an integration path is not at the boundary-layer edge. In this case, the boundary-layer edge velocity q_e in the integrand of δ_i^* assumes the value of the maximum q occurring in the path, which ensures a positive δ_i^*. These approaches guarantee continuous distributions of δ and δ_i^*.

The original Johnson–King model[15] was modified as follows. The suggestions by Johnson and Coakley[19] that enable the model to satisfy the law of the wall better under adverse pressure gradient are used. Also incorporated are the Savill–Gatski[20] modifications that deal with the anisotropicity of the eddy-viscosity field in three-dimensional boundary layers. Moreover, the constant 0.0168 in the outer eddy-viscosity formulation is replaced by a variable outer layer parameter derived by Leung and Squire,[21] which essentially relates the maximum eddy-viscosity value to the shape and skewness of the boundary-layer profile. The modified Johnson–King model has been tested in certain boundary-layer flows under an adverse pressure gradient [e.g., the National Aerospace Laboratory (NLR) swept wing flow[22]], and the results show that the modifications improved the predictions. Full details of these modifications and validation are given in the paper by Leung and Squire.[21]

IV. Result

In the high-Reynolds-number experiments, surface oil flow pictures were obtained at 7–13 deg incidences. The 13-deg picture is shown in Fig. 4. A widely accepted flow separation criterion is that the oil flow lines show a complete convergence, i.e., the streaks coalesce onto a single line. This complete convergence appears in the sidewall patterns at all incidences $\geq$ 8 deg, at least in the region near the wedge leading edge, meaning that incipient separation occurs at a wedge angle between 7 and 8 deg. Further away from the apex, the oil lines seem to run parallel to one another in a narrow band. This is what Kubota and Stollery called incomplete convergence. Moreover, the width of the band seems to be growing in the outboard direction, at least in the neighborhood of the complete convergence line. In the low-Reynolds-number experiments, Kubota and Stollery found from their oil flow pictures that incipient separation occurred at a wedge angle between 10 and 11 deg. They also observed a zone of incomplete convergence that continued from the complete convergence line in the outboard direction, and the width of the zone also grew. Their 13-deg incidence oil flow picture is shown in Fig. 4 alongside the high-Reynolds-number one.

As in the present high-Reynolds-number oil flows, the complete convergence lines in Kubota and Stollery's sidewall pictures move gradually away from the wedge as the angle of incidence is increased. Moreover, the difference in the angular positions of the convergence line and the inviscid shock, i.e. $\beta_c - \beta_s$ (angle of convergence line − shock angle), also rises with the wedge angle. Figure 5 shows the variation of $\beta_c - \beta_s$ with wedge angle for the two cases. It is also useful to measure and compare the inclination of the upstream influence line, which is drawn by connecting the points in the surface

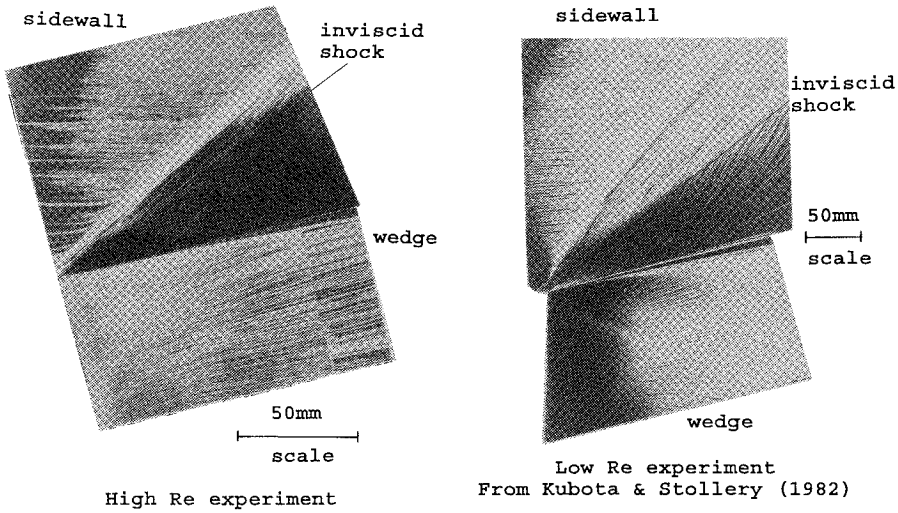

Fig. 4 Experimental oil flow pictures at 13-deg incidence.

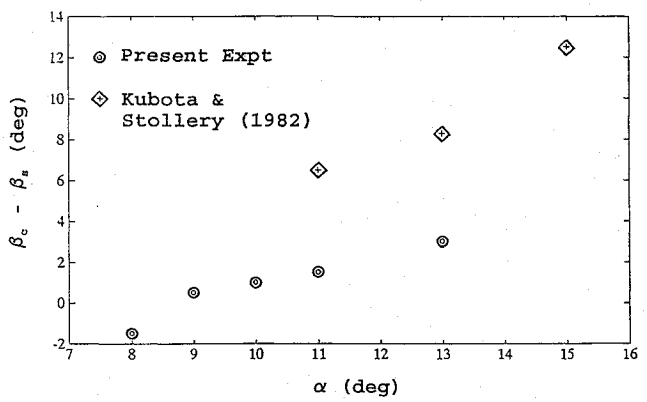

Fig. 5 Variation of angle between convergence line and inviscid shock with angle of incidence.

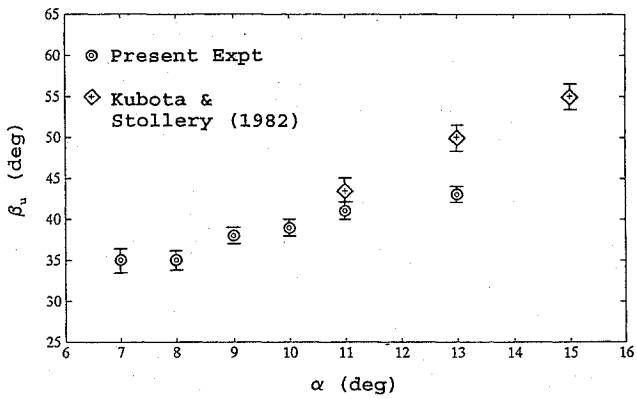

Fig. 6 Variation of upstream influence angle with angle of incidence.

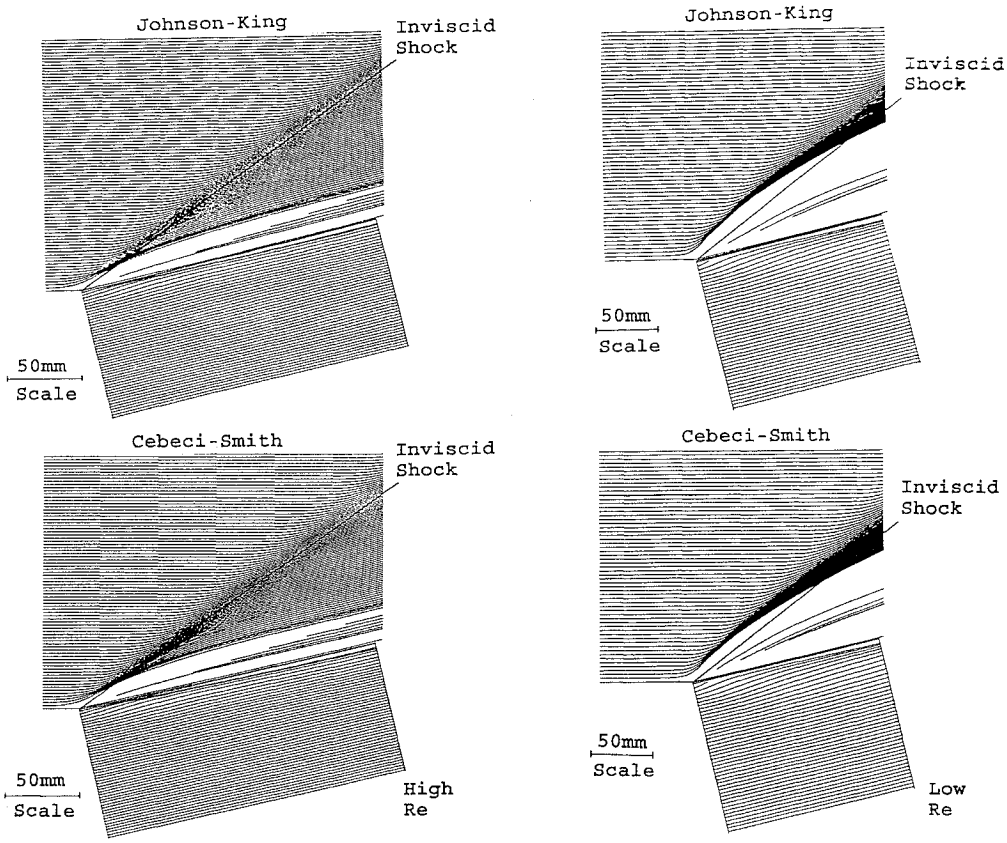

Fig. 7 Computed oil flow pictures at 13-deg incidence.

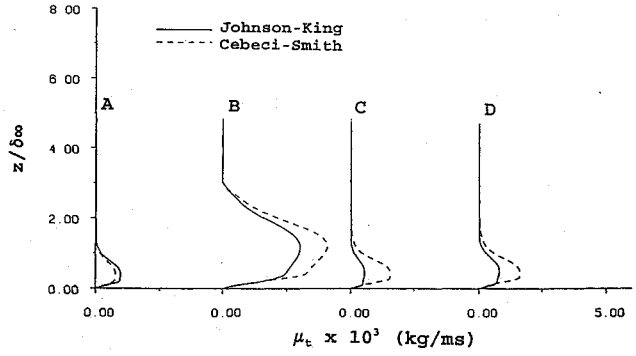

Fig. 8 Eddy-viscosity profiles at low-Reynolds-number and 13-deg incidence.

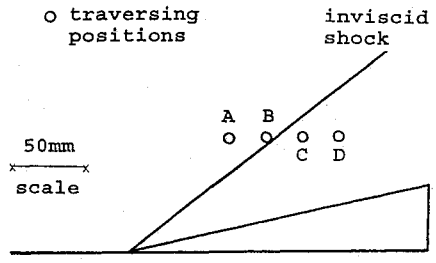

Fig. 9 Traversing positions at low-Reynolds-number and 13-deg incidence.

flow pictures where the oil streaks first show sign of turning. As shown in Fig. 6, at small incidences the upstream influence angle β_u in Kubota and Stollery's experiments is slightly higher than the present ones, and the difference grows with the wedge angle.

Owing to the shortage in computational resources, only simulations at 7 and 13 deg are performed for the two Reynolds number flows, and thus it is not possible to check the occurrence of incipient separation by the computations. The computed 13-deg incidence oil flows for both the high and low Reynolds numbers are shown in Fig. 7. General features of the experimental oil flows are shown by the computed pictures. For example, the sidewall convergence at 13-deg incidence is seen on both Reynolds-number simulations. The curvature of the convergence line shown by the experimental surface flow in the low-Reynolds-number 13-deg incidence case is clearly present in the computed picture. However, the deflection of the oil flow lines is slightly underpredicted. As to the wedge surface, in all of the computed pictures the oil flow lines on this surface turn at first towards the sidewall and then away from it, which agrees with the experiments. Complete convergence on this surface is seen at the higher Reynolds number cases, in accordance with experimental observations. For the low-Reynolds-number cases, however, in the computations no convergence line appears on the wedge, although the oil flows clearly run towards one another at the trailing edge especially for the 13-deg incidence. This suggests that the separated flow is more developed at the higher Reynolds-number at 13-deg incidence, i.e., incipient separation occurs at a lower incidence at the higher Reynolds number. The difference between using different turbulence models is not very significant, although the Johnson-King model predicts somewhat higher sidewall flow deflections in the low-Reynolds-number cases. Figure 8 shows the eddy-viscosity profiles at four different traversing positions indicated in Fig. 9. It can be seen that, despite the similarity in the flowfields produced by the two models, there exist considerable differences in the eddy-viscosity values. This supports the claim by Knight et al.[23] that the structure in this type of interaction flow is rather insensitive to the eddy-viscosity magnitude.

Surface static pressure has also been measured and computed. Figures 10 and 11 show, respectively, the experimental and computed surface pressure contours for the low-Reynolds-number case at 13-deg incidence. As seen the agreement is reasonable. The expected spreading of pressure rise over a finite distance is seen in both pictures. An approximately conical pattern is also noted. However, the upstream influence extent in the computed picture is smaller

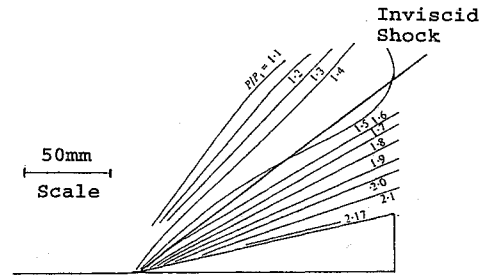

Fig. 10 Experimental surface pressure contours at low-Reynolds-number and 13-deg incidence (from Kubota and Stollery).

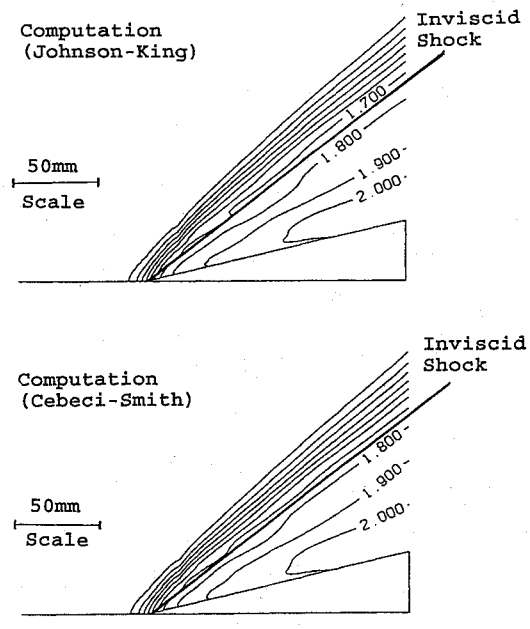

Fig. 11 Computed surface pressure contours at low-Reynolds-number and 13-deg incidence.

than the experimental one. As in the case of the oil flows, the effect of using different turbulence models is not marked.

V. Discussion

Upstream Influence

In an attempt to investigate the Mach number effect on the three-dimensional interaction, Lu et al.[7] related the upstream influence angle β_u and the inviscid shock angle β_s to the freestream Mach angle μ_∞ and found that their data for four sets of flow conditions collapse to a single curve:

$$\Delta\beta_u = 2.2\Delta\beta_s - 0.027\Delta\beta_s^2 \tag{1}$$

where $\Delta\beta_u = \beta_u - \mu_\infty$ and $\Delta\beta_s = \beta_s - \mu_\infty$

The value of the unit Reynolds number of their data set falls in the range $5.38–7.58 \times 10^7$/m and M_∞ spans from 2.47 to 3.95, whereas Re_{δ_∞} is kept approximately constant at 2×10^5 so as to eliminate the effect of this parameter. Figure 12 shows how the variation of $\Delta\beta_u$ with $\Delta\beta_s$ in the present and Kubota and Stollery's experiments compares with Eq. (1). As seen, there exists some difference between the experimental trends and Eq. (1), especially for Kubota and Stollery's case. Because the Mach number (2.47) in one of Lu et al.'s data set is close to the present and Kubota and Stollery's experiments, it would appear that the departure from Eq. (1) is due to the difference in Re_{δ_∞} (2.96×10^5 in the present case; 4.87×10^4 in Kubota and Stollery).

Incipient Separation

Settles and Dolling suggested that the conditions for incipient separation in three-dimensional shock/boundary interactions are similar to those in two dimensions if the proper coordinate frame

Table 1 Comparison of flow conditions at incipient separation in the two experimental cases and those predicted theoretically in Refs. 10 and 11

Case	R_θ	M_∞	α_s, deg	p_2/p_1	M_n	α_s, deg, Ref. 10	p_2/p_1, Ref. 10	p_2/p_1, Ref. 11
Kubota and Stollery	3.1×10^3	2.30	10.5 ±0.5	1.84	1.31	13.0 ±0.5	2.1	1.59 ±.02
Present (Leung and Squire)	2.0×10^4	2.45	7.5 ±0.5	1.6	1.23	8.5 ±0.5	1.68	1.50 ±0.2

normal to the shock is considered so that the Mach number normal to the shock M_n is the significant parameter in the determination of incipient separation. In two-dimensional flow Liu and Squire[24] have shown that incipient shock induced separation occurs at $M_\infty(\equiv M_n) = 1.3$, a value also arrived at by Zheltovodov et al.[25] However, in two-dimensional flow the effects of changes in Reynolds number on incipient separation are not clear. This is partly due to the difficulty in defining separation, but more importantly to the fact that there have been very few systematic investigations of the effects of Reynolds number using the same facility and criteria for incipient separation. In fact, in many investigations the method used to generate the shock means that it is impossible to change the Reynolds-number (see, for example, Atkin and Squire[26]). The recent theories of Dou and Deng[10] and of Zheltovodov et al.[11] mentioned earlier for swept interactions both predict a Reynolds number effect on incipient separation; the results from these predictions are given in Table 1 where they are compared with the present e cperimental results.

As can be seen, the experimental results and both theories show a decrease in pressure ratio for incipient separation for the present high-Reynolds-number tests as compared with the low-Reynolds-number tests of Kubota and Stollery. The theory of Zheltovodov et al. is independent of M_∞ so that the predicted increase in p_2/p_1 from 1.5 to 1.59 is entirely due to decrease in Re_θ; on the other hand the theory of Dou and Deng predicts an effect of both M_∞ and Re_θ, and it is estimated that of the predicted increase in p_2/p_1 from 1.68 to 2.1, 0.12 is due to the change in Mach number. Thus it would appear that for the present experiments the method of Zheltovodov et al. underpredicts the effect of change in Reynolds number, whereas that of Dou and Deng overpredicts it, but both predictions agree with the experimental results that separation occurs at lower pressure ratios with increase in Reynolds number based on momentum thickness. However, it must be noted that the two predictions are based on entirely different physical assumptions. That of Zheltovodov et al. uses a quasi-two-dimensional approach based on the free-interaction concept. Thus, in theory, the same effect of Reynolds number should be present in two-dimensional flow, yet, as mentioned earlier, there is no conclusive evidence for any Reynolds number effect in two-dimensional flow. The method of Dou and Deng assumes that separation occurs when the surface streamlines are parallel to the inviscid shock and calculates this condition by using Johnston's triangular model[27] for three-dimensional boundary layers. The constants in this model are fixed by the use of the Prandtl–Meyer angles in the outer part of the boundary layer and by a correlation of skin friction with Mach number for the inner part. Since this model uses a different definition of separation from that used here, we would not expect perfect agreement with the present experimental results. However, both methods suggest that the main effect of Reynolds number arises from the decrease in skin-friction coefficient with increase in Reynolds number. This possible importance of the level of the skin-friction coefficient, together with the fact, noted earlier, that the angular extent of upstream influence appears to decrease with increasing Re_θ, suggests that the thickness of the viscous sublayer and the thickness of the sonic layer play a dominant part in the determination of incipient separation. Basically an increase in Re_θ will result in a decrease in the relative thickness of the viscous and sonic layers, leading to a decrease in upstream influence and to an increase in pressure gradient. However, as the thickness of the sonic layer decreases, the importance of the supersonic part of the layer increases. This allows for changes

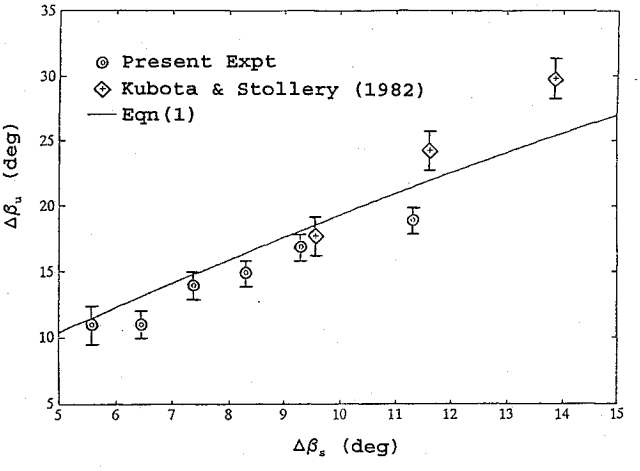

Fig. 12 Variation of referenced upstream influence angle with referenced inviscid shock angle.

in the upstream influence along the Mach waves in the outer part of the layer that, as pointed out by Stanbrook,[28] are less swept than the inviscid shock and so allow disturbances to propagate ahead of the shock. It would appear that the effect of Reynolds number on incipient separation noted here arises from the balance between these various conflicting influences. To clarify these effects in more detail, it would be interesting to study some of many other experimental results available for incipient separation. However, it is felt that such a study could only help if access was available to the full original results to ensure that exactly similar conditions are being used to determine incipient separation.

Inception Length

From a number of experimental results, Settles[6] found that the inception length was correlated by the equation

$$\left(\frac{L_i}{\delta_\infty}\right) Re_{\delta_\infty}^{1/3} \approx 1130 \cot \beta_s \tag{2}$$

at $M_\infty = 3$. The unit Reynolds numbers in these experiments are on the order of 10^7/m and 10^8/m (with $10^5 \leq Re_{\delta_\infty} \leq 10^6$). Later, Lu and Settles[29] performed another correlation from experimental data obtained in a larger Mach number range, $2.5 \leq M_\infty \leq 4.0$. (The Reynolds number values are given in Lu et al.,[7] which is mentioned earlier in this section.) In the correlation the normalized inception length shows the following trend within a certain range of β_s,

$$\frac{L_i}{\delta_\infty} = -43 + \frac{1680}{\beta_s} \qquad 20 \leq \beta_s \leq 35 \text{ deg} \tag{3}$$

Lu and Settles also observed that at larger inviscid shock angles L_i/δ_∞ flattened off at a value of 3. They commented that since the unit Reynolds number falls within a relatively narrow range of $5.38–7.58 \times 10^7$/m in their data set, the effect of unit Reynolds number in their correlation could not be explored and so Eq. (3) does not incorporate this parameter. Moreover, when Lu and Settles compared their $M_\infty = 2.95$ data with Eq. (2), which was obtained at Mach 3, they found significant discrepancies, especially at large β_s. The Reynolds numbers of the data sets are also quite close.

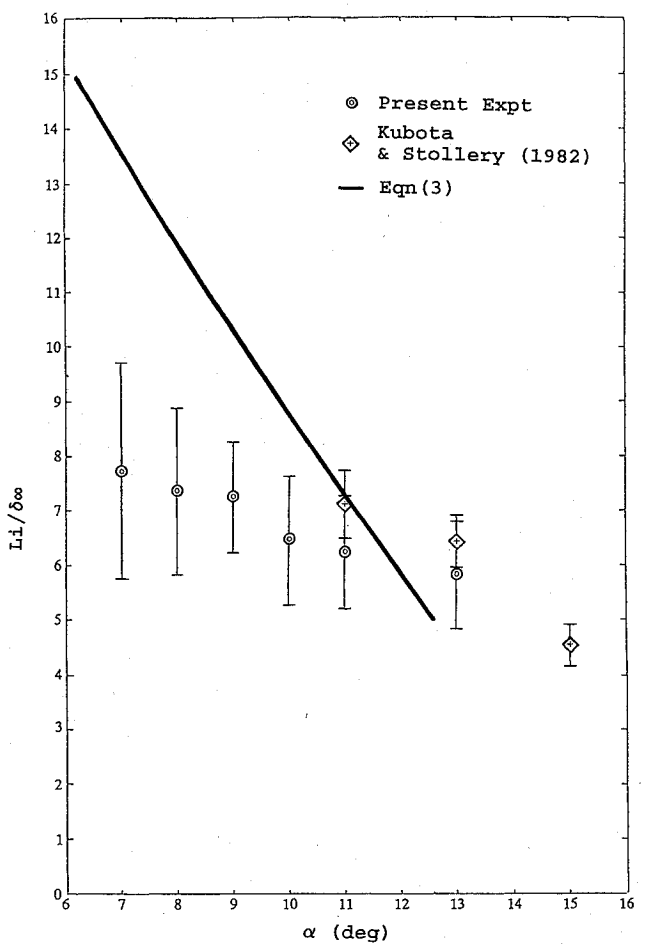

Fig. 13 Variation of normalized inception length with angle of incidence.

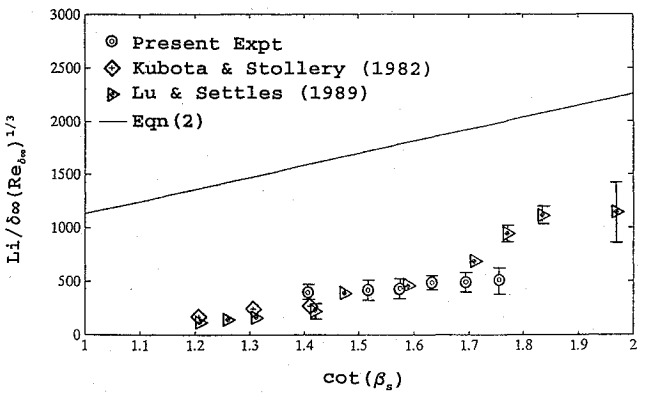

Fig. 14 Variation of L_i/δ_∞ $(\mathrm{Re}_{\delta_\infty})^{\frac{1}{3}}$ with $\cot\beta_s$.

The discrepancies are attributed largely to the fact that there exists certain arbitrariness in locating the inception region, which is where the upstream influence line departs from the asymptotic behavior in the far field. In fact, when Lu and Settles re-evaluated the inception lengths in the Mach 2.95 case using a more relaxed criterion, the results then agreed with the predictions by Eq. (2) at a 5% accuracy. They concluded that since the inception and the asymptotic regions merged gradually together, there seemed to be no natural criterion for determining the inception length. The actual criterion adopted was therefore not really important as long as one used it consistently for an entire data set.

The variation of L_i/δ_∞ with the wedge angle α in Kubota and Stollery's and the present experiments is plotted in Fig. 13. In both sets of experiments L_i/δ_∞ decreases with α. Equation (3) is also plotted, up to an inviscid shock angle of 35 deg, in Fig. 13 at the Mach number of the present experiments. The disagreement between Eq. (3) and the experiments is quite large at the lower end of α, and the equation predicts a much quicker fall of L_i/δ_∞ with α than was observed. Figure 14 shows how Eq. (2) compares the values of L_i/δ_∞ $(Re_{\delta_\infty})^{\frac{1}{3}}$ in the two experiments and also in the Mach 2.47 data set of Lu and Settles. It can be seen that Eq. (2) does not fit well with the data. However, it does seem that scaling with $(Re_{\delta_\infty})^{\frac{1}{3}}$ makes the data from the high- and low-Reynolds-number experiments collapse into a narrow band in the graph.

VI. Summary

The present investigation focuses on the Reynolds number effects of three-dimensional shock-wave/turbulent-boundary-layer interaction. Comparing two sets of flow at different Reynolds numbers but otherwise similar conditions, it is found that the upstream influence angle and the inception length normalized with boundary-layer thickness decrease with the Reynolds number. However, scaling the latter with $(Re_{\delta_\infty})^{\frac{1}{3}}$ removes considerably its Reynolds-number dependence. Moreover, it has also been seen that shock-induced separation on the sidewall happens more easily in the high-Reynolds-number case. Furthermore, the agreement between the computations and experiments is good, although the upstream influence in the oil flows and surface static pressure patterns is underpredicted. The calculated flowfield is shown to be insensitive to the eddy-viscosity values.

Acknowledgments

A grant by the Science and Engineering Research Council, which enabled the authors to use the University of London Computer Centre Convex C3840 computer, is gratefully acknowledged. The first author would also like to thank the Croucher Foundation of Hong Kong for the financial support towards his Ph.D. studies. The authors would like to thank W. N. Dawes for providing them the original Navier–Stokes solver, A. M. Savill for enlightening discussions on the Johnson–King model and its anisotropic modifications, and C. W. Hustad for performing the code modification on the isenthalpic flow assumption. They are also grateful to J. L. Stollery for his consent to the authors to reproduce the low-Reynolds-number experimental results performed by him and H. Kubota.

References

[1]Kubota, H., and Stollery, J. L., "An Experimental Study of the Interaction Between a Glancing Shock Wave and a Turbulent Boundary Layer," *Journal of Fluid Mechanics*, Vol. 116, March 1982, pp. 431–458.

[2]Alvi, F. S., and Settles, G. S., "Physical Model of the Swept Shock/Boundary-Layer Interaction Flowfield," *AIAA Journal*, Vol. 30, No. 9, 1992, pp. 2252–2258.

[3]Settles, G. S., and Dolling, D. S., "Swept Shock/Boundary-Layer Interactions Tutorial and Update," AIAA Paper 90-0375, Jan. 1990.

[4]Degrez, G., and Ginoux, J. J., "Surface Phenomena in a Three-Dimensional Skewed Shock Wave/Laminar Boundary Layer Interaction," *AIAA Journal*, Vol. 22, No. 12, 1984, pp. 1764–1769.

[5]Settles, G. S., and Lu, F. K., "Conical Similarity of Shock/ Boundary-Layer Interactions Generated by Swept and Unswept Fins," *AIAA Journal*, Vol. 23, No. 7, 1985, pp. 1021–1027.

[6]Settles, G. S., "On the Inception Lengths of Swept Shock-Wave/ Turbulent Boundary-Layer Interactions," *Proceedings of the IUTAM Symposium on Turbulent Shear Layer/Shock Wave Interactions* (Palaiseau, France), edited by J. Delery, Springer, Berlin, 1985, pp. 203–213.

[7]Lu, F. K., Settles, G. S., and Horstman, C. C., "Mach Number Effects on Conical Surface Features of Swept Shock-Wave/Boundary-Layer Interactions," *AIAA Journal*, Vol. 28, No. 1, 1990, pp. 91–97.

[8]Lowrie, B. W., "Cross-Flows Produced by the Interaction of a Swept shock wave with a Turbulent Boundary Layer," Ph.D. Thesis, Engineering Dept., Cambridge Univ., Cambridge, England, UK, Dec., 1965.

[9]Lu, F. K., "Semi-Empirical Extension of McCabe's Vorticity Model for Fin-Generated Shock-Wave Boundary-Layer Interactions," *Proceedings of 4th Asian Congress of Fluid Mechanics* (Hong Kong), Hong Kong Univ. Press, Hong Kong, 1989, pp. A170–A173.

[10]Dou, H., and Deng, X., "Prediction for the Incipient Separation of Fin-Generated Three-Dimensional Shock Wave Turbulent Boundary Layer Interactions," *Acta Aerodynamics Sinica*, Vol. 10, No. 1, 1992, pp. 1–10.

[11]Zheltovodov, A. A., Maksimov, A. I., and Shilein, E. K., "Development of Turbulent Separated Flows in the Vicinity of Swept Shock Waves," *The*

Interactions of Complex 3-D Flows, edited by A. M. Kharitonov, Akademia Nauk USSR, Inst. of Theoretical and Applied Mechanics, Novosibirsk, Russia, 1987, pp. 67–91.

[12]Dawes, W. N., "A Numerical Analysis of the Three-Dimensional Viscous Flow in a Transonic Compressor Rotor and Comparison with Experiment," *Journal of Turbomachinery*, Vol. 109, Jan. 1987, pp. 83–90.

[13]Holmes, S. C., and Squire, L. C., "Numerical Studies of Supersonic Flow over a Compression Corner," *Aeronautical Journal*, Vol. 96, No. 953, 1992, pp. 87–95.

[14]Cebeci, T., and Smith, A. M. O., *Analysis of Turbulent Boundary Layers* Academic, New York, 1974.

[15]Johnson, D. A., and King, L. S., "A New Turbulence Closure Model for Boundary Layer Flows with Strong Adverse Pressure Gradients and Separation," AIAA Paper 84-0175, Jan. 1984.

[16]Buleev, N. I., "Theoretical Model of the Mechanism of Turbulent Exchange in Fluid Flows," *Teploperedacha*, USSR Academy of Sciences, Moscow, Russia, 1962, pp. 64–98; see also *AERE Translation 957*, Atomic Energy Research Establishment, Harwell, England, UK, 1963.

[17]Hung, C. M., and MacCormack, R. W., "Numerical Solution of Three-Dimensional Shock Wave and Turbulent Boundary-Layer Interaction," *AIAA Journal*, Vol. 16, No. 10, 1978, pp. 1090–1096.

[18]Cambier, L., and Escande, B., "Calculation of a Three-Dimensional Shock Wave-Turbulent Boundary Layer Interaction," *AIAA Journal*, Vol. 28, No. 11, 1990, pp. 1901–1908.

[19]Johnson, D. A., and Coakley, T. J., "Improvement to a Nonequilibrium Algebraic Turbulence Model," *AIAA Journal*, Vol. 28, No. 11, 1990, pp. 2000–2003.

[20]Savill, A. M., Gatski, T. B., and Lindberg, P. A., "A Pseudo-3D Extension to the Johnson and King Model and Its Application to the EuroExpt S-duct Geometry," *Proceedings of 1st ERCOFTAC Workshop on Numerical Simulation of Unsteady Flows and Transition to Turbulence* (Lausanne), edited by O. Pirroneau, W. Rodi, I. L. Ryhming, A. M. Savill, and T. U. Truong, Cambridge Univ. Press, Cambridge, England, UK, 1992, pp. 158–165.

[21]Leung, A. W. C., and Squire, L. C., "A Comparison of Several Eddy-Viscosity Models in Two and Three Dimensional Boundary Layer Flows," *Aeronautical Journal*, Vol. 98, No. 973, 1994, pp. 73–82.

[22]Van den Berg, B., and Elsenaar, A., "Measurements in a Three-Dimensional Incompressible Turbulent Boundary Layer in an Adverse Pressure Gradient Under Infinite Swept Wing Conditions," National Aerospace Lab. NLR TR 72092U, Amsterdam, The Netherlands, Aug. 1972.

[23]Knight, D. D., Horstman, C. C., Shapey, B., and Bogdonoff, S. M., "The Flowfield Structure of the 3-D Shock Wave-Boundary Layer Interaction Generated by a 20 Degree Sharp Fin at Mach 3," AIAA Paper 86-0343, Jan. 1986.

[24]Liu, X., and Squire, L. C., "An Investigation of Shock/Boundary-Layer Interaction on Curved Surfaces at Transonic Speeds," *Journal of Fluid Mechanics*, Vol. 187, Feb. 1988, pp. 467–486.

[25]Zheltovodov, A. A., Maksimov, A. I. and Shilein, E. K., "3-D Interactions of Swept Shock Waves with Turbulent Boundary Layers in Corner Configurations," Inst. of Theoretical and Applied Mechanics, Preprint No. 34–86, USSR Academy of Sciences, Novosibirsk, Russia, 1986.

[26]Atkin, C. J., and Squire, L. C., "A Study of the Interaction of a Normal Shock Wave with a Turbulent Boundary Layer at Mach Numbers Between 1.30 and 1.55," *European Journal of Mechanics B/Fluids*, Vol. 11, 1992, pp. 92–118.

[27]Johnston, J. P., "On the Three-Dimensional Boundary-Layer Generated by Secondary Flow," *Journal of Basic Engineering*, Vol. 82, 1960, pp. 233–248.

[28]Stanbrook, A., "An Experimental Study of the Glancing Interaction Between a Shock Wave and a Turbulent Boundary Layer," British Aeronautical Research Council, CP 555, July 1960.

[29]Lu, F. K., and Settles, G. S., "Inception Length to a Fully-Developed Fin-Generated Shock Wave Boundary-Layer Interaction," AIAA Paper 89-1850, June 1989.